3. Proposed Deep Learning Model

In this study, it is assumed that the ARIS's 3D spatial movement is characterized by the RWMM [41]. Samples of its positions may be obtained from a homogeneous 3D Poisson process and the system model discussed in the preceding sections. For the purpose of explanation, we additionally assume that the ARIS moves spatially in a 3D cylinder, as shown in Figure 6. As a result, every element of the cylindrical coordinate of T can be produced from a uniform distribution which are as follows [27]: $\bar{\eta}[\text{dB}] = [5-\epsilon_\eta, 5+\epsilon_\eta]$, $\omega_T \sim \varkappa(0, 2\pi)$, $m_c = [2-\epsilon_m, 2+\epsilon_m]$, $\zeta_c = [2.5-\epsilon_\zeta, 2.5+\epsilon_\zeta]$, $N = [15/20/30 - \epsilon_N, 15/20/30 + \epsilon_N]$, $v = [2.7-\epsilon_v, 2.7+\epsilon_v]$, $r_T \sim 0.5\sqrt{\varkappa(0,1)}$, $h_T \sim \varkappa(0,1)$, $\delta_c = [1-\epsilon_\delta, 1+\epsilon_\delta]$, and $A_{\text{cth}} = [5-\epsilon_{A_c}, 5+\epsilon_{A_c}]$, respectively. It should be observed that distances among nodes in the suggested framework are now RVs due to the incorporation of 3D movement. This makes it impossible to derive the system OP specified in (7), mostly due to the multivariate confluent hypergeometric function. To get over this obstacle, we approach the task of locating the system OP in supervised learning. Specifically, we produce a data set that thoroughly describes the system under consideration. This dataset is used to train the generated BiLSTM model, enabling it to estimate the OP with high accuracy in different system configurations.

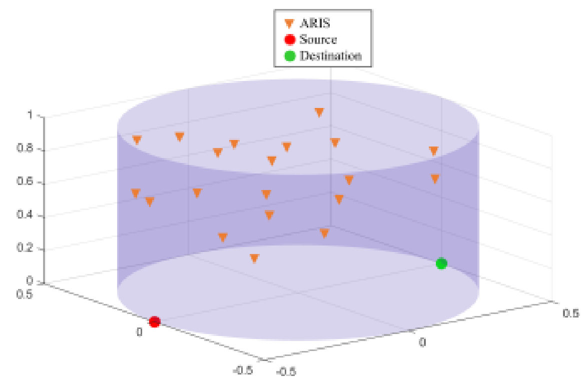

Figure 6. The architecture of the 3D spatial movement of the ARIS system.

3.1. 3D Modeling of Spatial Movement and Datasets Preparation

It is assumed that the azimuth, radial distance, and height of the cylindrical coordinate of T are represented by the symbols φ_T, r_T, and q_T, respectively. We take into consideration a unit normalization cylinder, that is, $\varphi_T \in [0, 2\pi]$, $r_T \in [0, 0.5]$, and $q_T \in [0, 1]$, without losing generality. This results in the conversion of R's 3D Cartesian coordinates, (x_T, y_T, z_T), to $x_T = r_T sin\varphi_T$, $y_T = r_T cos\varphi_T$, and $z_T = q_T$. Given the 3D Cartesian coordinates of the source and destination as (−0.5, 0, 0) and (0.5, 0, 0), respectively, one can compute the distance between two nodes using the following formula: $d_{ab} = \sqrt{(x_a - x_b)^2 + (y_a - y_b)^2 + (z_a - z_b)^2}$ where $\{a, b\} \in \{\text{source}, \text{destination}, \text{T}\}$.

In this study, the preparation of datasets, χ, is involved in the proposed ARIS system. Specifically, in the datasets, χ includes samples d_s of the information gathered from the AIRS system where the input–output connection could be $Data[d_s] = [\text{F}[d_s], P_{d_j}^{d_s}]$, where $\text{F}[d_s]$ represents the feature vector involving with all inputs characterized as shown in Table 1. However, this work has enough simulation samples to produce highly accurate outage performance estimates. After generating real-value CSI sets for each feature vector $\text{F}[d_s]$, the simulation runs a Monte Carlo. To build the data set, we generate 20^3 samples in total, i.e., $Data[d_s]$, $d_s = 1, ..., 20^3$, for utilizing the proposed model. After that, it splits the data set with ratios of 80%, 10%, and 10% for the training set Tr_χ, validation set Va_χ, and test set Te_χ. Through the mean-squared error (MSE), the accuracy of such a forecast may be assessed using (25).

Table 1. Inputs for the BiLSTM training and testing.

Parameters	Input Value
$\eta[dB]$	$-10\sim20$
φ_T	1
r_T	1
q_T	1
m_{St}	2.5
m_{tD}	2.5
ζ_c	2.5
N	15, 20, 30
v	1
h_T	1
δ_{St}	1
δ_{tD}	1
ζ_{St}	3
ζ_{tD}	3
A_{cth}	5

This from the paper of Rahman et al.